AMSE JOURNALS-AMSE IIETA publication-2017-Series: Advances A; Vol. 54; N°2; pp 153-168
Submitted Feb. 25, 2017; Revised May 01, 2017; Accepted Jun. 02, 2017

Analysis of the Responses to Typical Electromagnetic Excitations in TD-AEM Systems

Bing Guo*, Yiming Zhang

Faculty of Information Technology, Beijing University of Technology, Beijing 100124, China
(guobing116633@163.com)

Abstract

To help in the comparison of excitation sources for time-domain airborne electromagnetic (TD-AEM) systems, we develop an heuristic model of the response of the ground, represented by a conducting loop. For our comparison, our model includes the system waveforms. This model also includes a reception interval for on-time measurements, allowing the simulation and analysis of different electrical targets in both on-time and off-time. The results show that, for high-resistance targets, the use of the rectangular pulse excitation has the greatest response intensity during the off-time period, and for low-resistance targets, the use of the half-sine or the triangular pulse excitation has a higher signal-to-noise ratio during the on-time period. Results also show the influence of the pulse width on the response and may help in the selection of the pulse width while designing a survey.

Key words

AEM, Excitation waveform, Free space loop coil model, Signal to noise ratio.

1. Introduction

A TD-AEM system has the advantages of being fast, flexible, and efficient and has become a popular system in mineral resources exploration [1-2]. The system is widely used in mineral resources exploration, hydrogeological investigations, and for unexploded ordnance detection [3-6]. A typical TD-AEM exploration system uses a transmitting coil to generate a pulsed magnetic field (primary field), which generates eddy currents in the subsurface and then stimulates an

inductive magnetic field (secondary field) (Figure 1). Finally, the system analyzes this secondary field to determine the location of the underground ore.

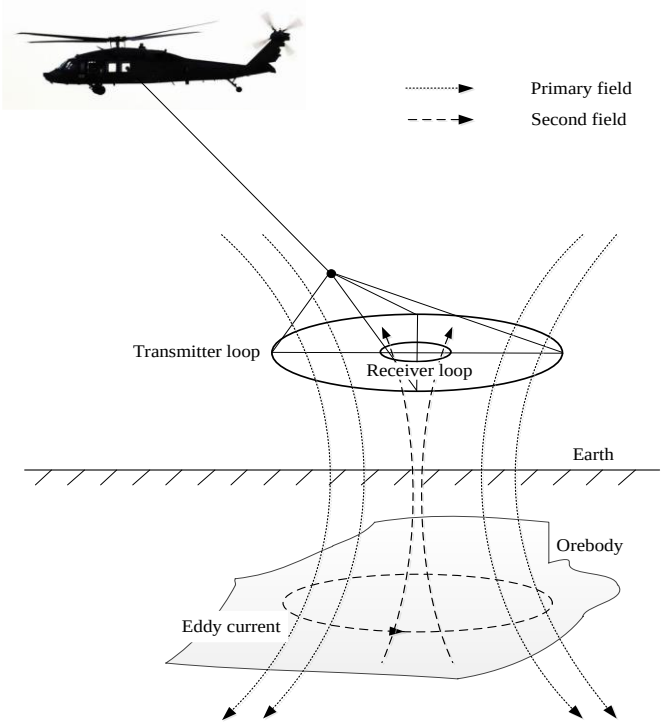

Fig.1. TD-AEM Operating Principle

At present, the time-domain electromagnetic (TDEM) transmitting waveform is mainly a square wave, a trapezoidal wave, a half-sine wave, or a triangular wave, while the measurements are principally observed in the absence of transmitting current (transmitting current I(t)=0), the so-called off-time observation. However, one of the biggest drawbacks of off-time observation is that due to the high time constant of a high-conductivity target, the eddy current decay is very slow, resulting in a weak secondary field, while a high-conductivity target represents the most valuable high-grade ore. Although the early GeoTech's VTEM system had a function for obtaining B through the dB/dt integral to improve the sensitivity [7], the problem of the weak response for high-conductivity targets has not been fundamentally solved.

Many of the international and recently-developed advanced AEM systems have an on-time detection function, that is, the secondary field is collected during the transmitting current ($I(t) \neq 0$). Examples of these systems include CGG's GeoTEM and MegaTEM fixed-wing systems with a half-sine current [8], Aeroquest's AeroTEM rotor system with a triangular wave [9], and GeoTech's VTEM-Plus rotor system with an approximately trapezoidal wave [10]. Therefore, it is of great

significance to study the principles that govern the on-time and off-time transient responses of different excitation sources to obtain a suitable design and system optimization and to achieve appropriate results. The present study focuses mainly on the influence of the excitation source on the trapezoidal pulse source [11-14]. The impact of various excitation sources on the response, especially the on-time detection, has not been reported in the literature.

Liu reported the response of the step, square wave, trapezoidal wave, triangular wave, and half-sine wave during the off-time and the response model was the exponential attenuation of the conductor loop in free space [15]. In this paper, the response of various excitation sources during off-time are discussed more in-depth and the conducting loop model [16] is extended to the response during the on-time period. On this basis, many important principles of on-time response are revealed, which can provide theoretical guidance for future TD-AEM system calibration and the design of systems with on-time measurement functions.

2. Typical Excitation Response

The TD-AEM system response model is shown in Fig. 2, where $I(t)$ is the transmitting current, $i(t)$ is the conducting loop induced current, $V(t)$ is the receiving coil response voltage, and R and L are the loop resistance and inductance respectively. The waveform excitation response mentioned below refers to the voltage response (dB/dt) captured by the receiver coil [16]. There are four typical pulse excitation shapes, including rectangular, trapezoidal, triangular, and half-sine. In order to facilitate a theoretical comparison, the step current is also discussed. In the following discussion, the impulse response function of the system is derived for the response of the step current. Subsequently, the impulse response function is convolved with each excitation source to obtain the corresponding system response. The response of the ground is represented as an electrical circuit, in the same way as Grant and West [17], shown on Figure 2.

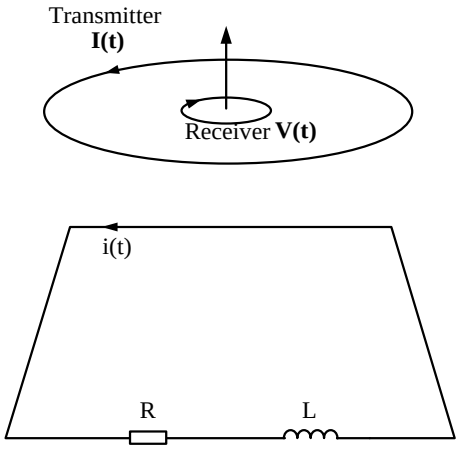

Fig.2. Free Space Loop Coil Response Model

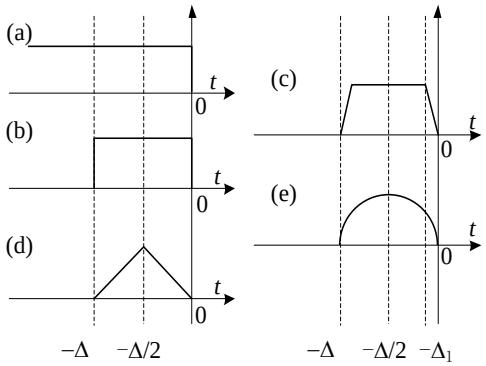

Fig.3. Typical Excitation Shape

The step current shown in Figure 3 (a) can be expressed as:

$$I_{step}(t)=I_o[1-u(t)] \tag{1}$$

where I_o is the peak current and $u(t)$ is the unit step function [14]. Based on the model shown in Figure 2, the response of the step current is given as:

$$V_{step}(t)=a\delta(t)-\frac{a}{\tau}e^{-t/\tau}u(t) \tag{2}$$

where $a=-M_{TL}M_{LR}I_o/L$, M_{TL} is the mutual inductance of the transmitting coil and the free space loop coil, M_{LR} is the mutual inductance of the free space loop coil and the receiving coil [14], and $\tau=L/R$ is the loop coil time constant.

$$V(t)=I(t)*h(t) \tag{3}$$

The system impulse response can be obtained by substituting (1) and (2) into equation (3).

$$h(t)=-a\delta'(t)+\frac{a}{\tau}\delta(t)-\frac{a}{\tau^2}e^{-t/\tau}u(t) \tag{4}$$

When the input current is $I(t)$, the corresponding system response is obtained as:

$$V(t)=-aI'(t)+\frac{a}{\tau}I(t)-\frac{a}{\tau^2}e^{-t/\tau}\int_{-\infty}^{t}I(\lambda)e^{\lambda/\tau}d\lambda \tag{5}$$

The time domain of each excitation source in Figure 3 is expressed as follows:

$$I_{square}(t)=u(t+\Delta)-u(t) \tag{6}$$

$$I_{trapezoidal}(t)=\frac{1}{\Delta_1}(t+\Delta)u(t+\Delta)-\frac{1}{\Delta_1}(t+\Delta-\Delta_1)u(t+\Delta-\Delta_1)-\frac{1}{\Delta_1}(t+\Delta_1)u(t+\Delta_1)+\frac{1}{\Delta_1}tu(t) \tag{7}$$

$$I_{half\text{-}sine}(t)=\sin\frac{\pi}{\Delta}(t+\Delta)u(t+\Delta)+\sin\frac{\pi}{\Delta}tu(t) \tag{8}$$

$$I_{triangular}(t)=\frac{2}{\Delta}(t+\Delta)u(t+\Delta)-\frac{4}{\Delta}(t+\frac{\Delta}{2})u(t+\frac{\Delta}{2})+\frac{2}{\Delta}tu(t) \tag{9}$$

The equations (6) to (9) are substituted into the equation (5), and the full-time domain response of each excitation source is obtained as follows:

$$V_{square}(t)=-a\left[\delta(t+\Delta)-\delta(t)\right]+\frac{a}{\tau}e^{-t/\tau}\left[e^{-\Delta/\tau}u(t+\Delta)-u(t)\right] \tag{10}$$

$$V_{trapezoidal}(t)=-\frac{a}{\Delta_1}e^{-t/\tau}\left[e^{-\Delta/\tau}u(t+\Delta)-e^{-(\Delta-\Delta_1)/\tau}u(t+\Delta-\Delta_1)-e^{-\Delta_1/\tau}u(t+\Delta_1)+u(t)\right] \tag{11}$$

$$V_{half\text{-}sine}(t)=\frac{\pi a}{\Delta}\frac{1}{1+\left(\frac{\Delta}{\pi\tau}\right)^2}\left(\cos\frac{\pi}{\Delta}t-\frac{\Delta}{\pi\tau}\sin\frac{\pi}{\Delta}t\right)\left[u(t+\Delta)-u(t)\right]-\frac{\pi a}{\Delta}\frac{e^{-\Delta/\tau}}{1+\left(\frac{\pi\tau}{\Delta}\right)^2}\left[e^{-\Delta/\tau}u(t+\Delta)+u(t)\right] \tag{12}$$

$$V_{triangular}(t)=\frac{-2a}{\Delta}e^{-t/\tau}\left[e^{-\Delta/\tau}u(t+\Delta)-2e^{-\Delta/2\tau}u(1+\frac{\Delta}{2})+u(t)\right] \tag{13}$$

3. Receiver Response Signal During Off-Time

3.1 Initial Response Value

From the equations (2) and (10) to (13), the response of the receiving coil during the off-time (t>0) is:

$$V_{step}(t) = -\frac{a}{\tau} e^{-t/\tau} \tag{14}$$

$$V_{square}(t) = \frac{a}{\tau} e^{-t/\tau} (e^{-\Delta/\tau} - 1) \tag{15}$$

$$V_{trapezoidal}(t) = -\frac{a}{\Delta_1} e^{-t/\tau} \left[e^{-\Delta/\tau} (1 - e^{-\Delta_1/\tau}) + 1 - e^{-\Delta_1/\tau} \right] \tag{16}$$

$$V_{half\text{-}sine}(t) = -\frac{\pi a}{\Delta} \frac{e^{-t/\tau}}{1 + \left(\frac{\pi\tau}{\Delta} \right)^2} \left(e^{-\Delta/\tau} + 1 \right) \tag{17}$$

$$V_{triangular}(t) = -\frac{2a}{\Delta} e^{-t/\tau} \left(1 - e^{-\Delta/2\tau} \right)^2 \tag{18}$$

By calculating the limits for (14) - (18) respectively, the off-time initial response values are obtained as follows:

$$V_{step}(0^+) = \lim_{t \to 0^+} V_{step}(t) = -\frac{a}{\tau} \tag{19}$$

$$V_{square}(0^+) = \lim_{t \to 0^+} V_{square}(t) = \frac{a}{\tau} (e^{-\Delta/\tau} - 1) \tag{20}$$

$$V_{trapezoidal}(0^+) = \lim_{t \to 0^+} V_{trapezoidal}(t) = -\frac{a}{\Delta_1} \left[e^{-\Delta/\tau} (1 - e^{\Delta_1/\tau}) + 1 - e^{\Delta_1/\tau} \right] \tag{21}$$

$$V_{half\text{-}sine}(0^+) = \lim_{t \to 0^+} V_{half\text{-}sine}(t) = -\frac{\pi a}{\Delta} \frac{1}{1 + \left(\frac{\pi\tau}{\Delta} \right)^2} \left(e^{-\Delta/\tau} + 1 \right) \tag{22}$$

$$V_{triangular}(0^+) = \lim_{t \to 0^+} V_{triangular}(t) = -\frac{2a}{\Delta} \left(1 - e^{-\Delta/2\tau} \right)^2 \tag{23}$$

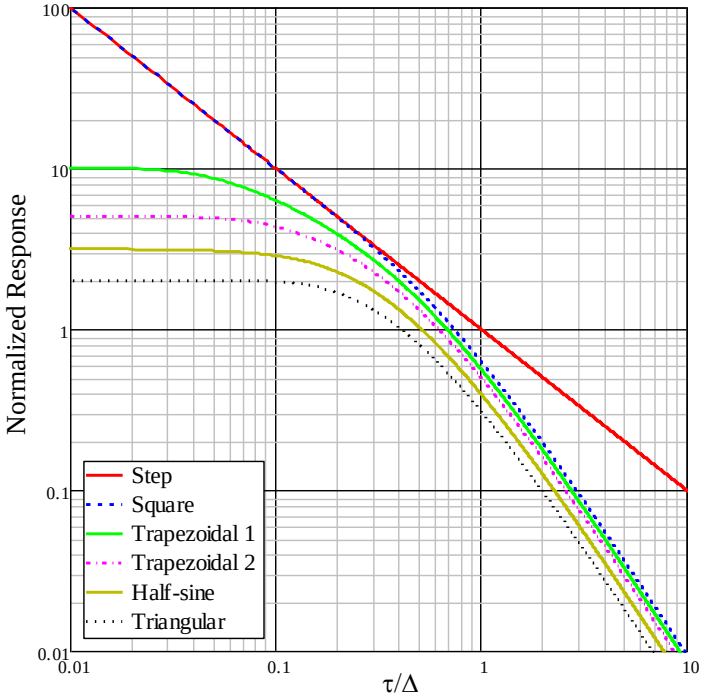

Fig.4. Initial Value of Off-Time Response

By normalizing (19) - (23) on $-a/\Delta$, the off-time initial response value varies with τ/Δ as shown in Figure 4, where the ratio of the edge width and the pulse width of Trapezoidal 1 and Trapezoidal 2 are 0.1 and 0.2 respectively.

3.2 Discussion of the Initial Response Value

It can be seen from Fig. 4 that the initial value of the response signal is affected by τ/Δ. The influences of various values for τ/Δ are discussed in the flowing section.

When τ/Δ is small:

① When $\tau/\Delta<0.1$, the initial values of the step excitation and the square wave excitation tend to be identical and the initial response value is inversely proportional to τ/Δ. Therefore, in the off-time period, for low-conductivity targets, the excitation effect of the square wave is the same as the excitation effect of the step wave, and its value is the highest for all the responses.

② The excitation responses of the trapezoidal, half-sine, and triangular excitations are close to their respective limits when τ/Δ is small, that is, the initial response of the three excitation sources is independent of τ/Δ. Normalized limit of (21) - (23) can be obtained as:

$$\lim_{\tau/\Delta\to 0}\left|\frac{V_{trapezoidal}(0^+)}{a/\Delta}\right|=\frac{\Delta}{\Delta_1} \tag{24}$$

$$\lim_{\tau/\Delta\to 0}\left|\frac{V_{half\text{-}sine}(0^+)}{a/\Delta}\right|=\pi \tag{25}$$

$$\lim_{\tau/\Delta\to 0}\left|\frac{V_{triangular}(0^+)}{a/\Delta}\right|=2 \tag{26}$$

As can be seen from (24), when Δ is constant, the smaller the edge time Δ_1 of the trapezoidal wave, the stronger the response signal is. As can be seen from (25) - (26), the initial value of the half-sine is π/2 times the initial value of the triangular wave but it is far less than the trapezoidal wave response.

When τ/Δ is large:

① When τ/Δ>1.0, the response amplitude of the step excitation results in a first-order decrease, and the response amplitude of the other pulse excitation results in a second-order decrease. The results show that, when detecting high-conductivity targets during off-time, the response amplitude of the trapezoidal, triangular, and half-sine waves are relatively small. If the response amplitude has to be increased, the excitation amplitude has to increase or the frequency of the excitation source has to be reduced. When the frequency is reduced by half, the signal amplitude becomes 4-fold.

② When τ/Δ>1.0, the response curves are parallel to each other, that is, the response ratio of the various pulse excitation waves is constant when τ/Δ is large. When using the square wave signal as a reference, the ratios of (20) - (23) to the reference are as follows:

$$\lim_{\tau/\Delta\to 0}\left|\frac{V_{trapezoidal}(0^+)}{V_{square}(0^+)}\right|=\lim_{\tau/\Delta\to 0}\left[\frac{\tau}{\Delta_1}\frac{1-e^{-\Delta_1/\tau}+e^{-\tau/\Delta}(1-e^{\Delta_1/\tau})}{1-e^{-\tau/\Delta}}\right]=1-\frac{\Delta_1}{\Delta} \tag{27}$$

$$\lim_{\tau/\Delta\to 0}\left|\frac{V_{half\text{-}sine}(0^+)}{V_{square}(0^+)}\right|=\lim_{\tau/\Delta\to 0}\left[\frac{\pi\tau}{\Delta}\frac{1+e^{-\Delta/\tau}}{1+\left(\frac{\pi\tau}{\Delta}\right)^2}\frac{1}{1-e^{-\Delta/\tau}}\right]=\frac{2}{\pi} \tag{28}$$

$$\lim_{\tau/\Delta\to 0}\left|\frac{V_{triangular}(0^+)}{V_{square}(0^+)}\right|=\lim_{\tau/\Delta\to 0}\left[\frac{2\tau}{\Delta}\frac{\left(1-e^{-\Delta/2\tau}\right)^2}{1-e^{-\Delta/\tau}}\right]=\frac{1}{2} \tag{29}$$

The following is a further discussion of the physical meanings of these ratios. When t>0, $\Delta/\tau \to 0$, the system's response (5) is simplified as:

$$V(t) = -\frac{a}{\tau^2} e^{-t/\tau} \int_{-\Delta}^{0} I(\lambda) d\lambda \tag{30}$$

where the integral term is the area surrounded by the excitation waveform and the time axis. It can be seen that the initial value of the off-time response is proportional to the area enclosed by the excitation waveform and the time axis when τ/Δ is large. The equations (27) - (29) represent this principle and the results show that by increasing the area enclosed by the excitation waveform and the time axis of the area, the initial response value can be improved. In other words, it is shown that increasing the amplitude and decreasing the frequency increases the signal amplitude.

③ When the edge of the trapezoidal wave is steep, the signal increases slightly due to the increase in the area enclosed by the time axis but in general, the edge time is negligible compared to the time of the whole pulse, that is, $1-\Delta_1/\Delta \approx 1$; Therefore, even if the edge is very steep, the response signal will not change much.

④ When $\tau/\Delta=0.4$, the half-sine and triangular waves achieve the best excitation effects (closest to the step response); Therefore, the optimal frequency should be selected when detecting a target with different conductivities. The optimal excitation pulse width of the trapezoidal wave is related to the edge; the steeper the edge, the smaller the ratio of the time constant to the optimal pulse width is. The square excitation waveform does not result in the optimal pulse width; the greater the pulse width, the closer the response amplitude to the step signal is.

4. Receiver Response Signal during On-Time

From the above discussion, it is evident that the decrease in conductivity causes the time constant of the target to decrease and the inductive signal is rapidly attenuated during the off-time. Therefore, these excitation sources are very efficient for measuring low-conductivity targets but are not ideal for high-conductivity targets. The main reason is that if the target conductivity is high, the eddy currents generated by the front edge of the excitation waveform in the target body and the eddy currents generated at the trailing edge of the excitation waveform cancel each other out, resulting in a significant reduction in the off-time response. Additionally, by increasing the compensation coil can reduce the dynamic range of the receiving circuit requirements, so that

capture on-time signal becomes feasible [10]. Therefore, it is necessary to study the characteristics of the on-time response.

4.1 Definition of the On-Time Receiving Interval

By normalizing the amplitude of (10) - (13) on $-a/\Delta$ and normalizing the time t on pulse width Δ, the time domain responses of various excitation waveforms are obtained as shown in Figure 5, where the loop time constant $\tau=\Delta$ and the trapezoidal wave $\Delta_1/\Delta=0.05$.

As shown in Figure 5, the response of the square excitation decays exponentially over the entire on-time period and the definition of the on-time signal reception interval is $(-\Delta, 0)$. The trapezoidal excitation response changes drastically at the rising and falling edges and the response amplitude is high. The trapezoidal excitation edge time is very short, during which the received signal is affected by the coil transition process and an accurate secondary field signal cannot be obtained. Therefore, the on-time acquisition region of the trapezoidal excitation response is defined as $(-\Delta+\Delta_1, -\Delta_1)$. The half-sine excitation response does not mutate during the on-time period; therefore, the on-time signal acquisition interval of the half-sine excitation response is defined as $(-\Delta, 0)$. The triangular excitation response has one mutation in the on-time interval and the amplitude increases with the mutation; therefore, the on-time signal acquisition interval of the triangular excitation is set to $(-\Delta/2, 0)$.

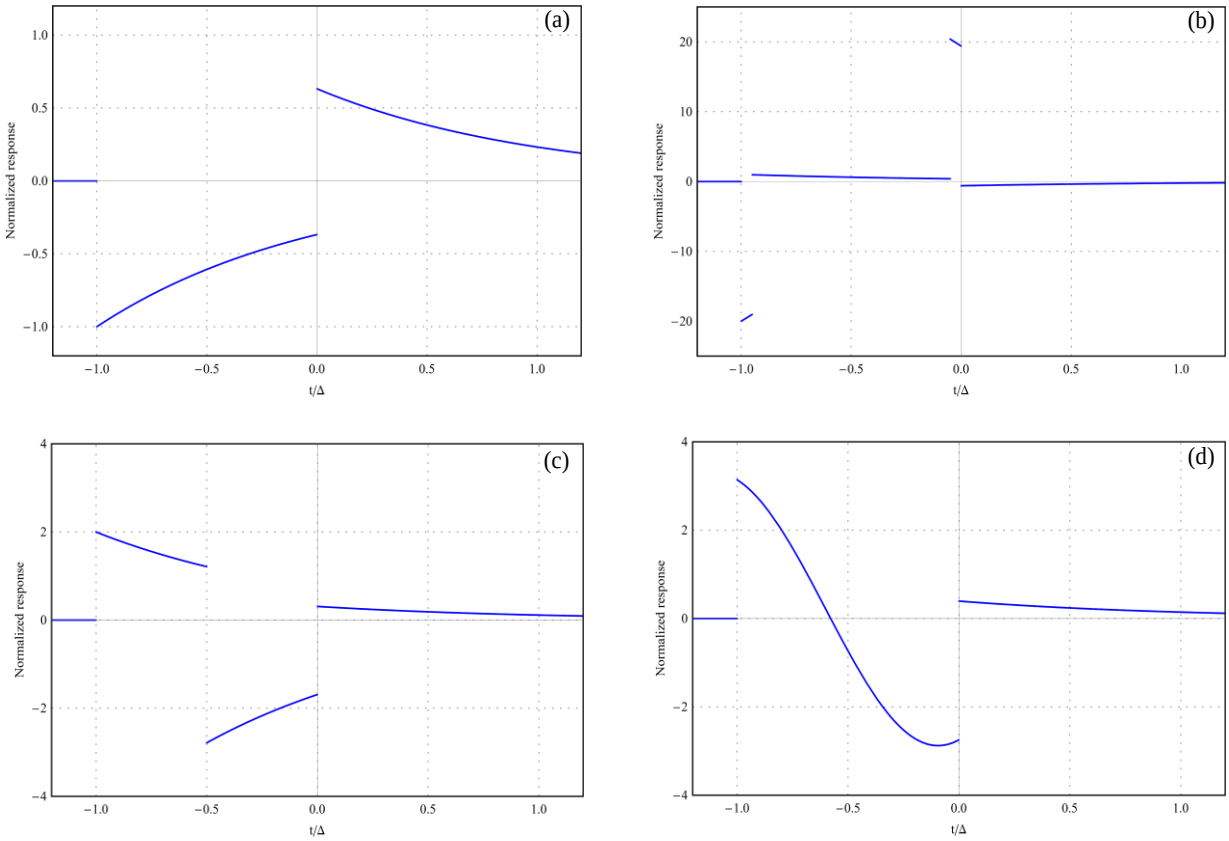

Fig.5. Pulse Responses of Different Excitations in the Time Domain, Where Part A Is Square Excitation Response, Part B Is Trapezoidal Excitation Response, Part C Is Triangular Excitation Response, and Part D Is Half-Sine Excitation Response.

4.2 On-Time Initial Response Value

According to (10) to (13), the response of each excitation waveform in the on-time acquisition interval is as follows:

$$V_{square}(t)=\frac{a}{\tau}e^{-(t+\Delta)/\tau},(-\Delta<t<0) \tag{31}$$

$$V_{trapezoidal}(t)=-\frac{a}{\Delta_1}e^{-(t+\Delta)/\tau}(1-e^{\Delta_1/\tau}),(-\Delta+\Delta_1<t<-\Delta_1) \tag{32}$$

$$V_{half\text{-}sine}(t)=\frac{\pi a}{\Delta}\left[\frac{1}{1+\left(\frac{\Delta}{\pi\tau}\right)^2}\left(\cos\frac{\pi}{\Delta}t-\frac{\Delta}{\pi\tau}\sin\frac{\pi}{\Delta}t\right)-\frac{e^{-(t+\Delta)/\tau}}{1+\left(\frac{\pi\tau}{\Delta}\right)^2}\right],(-\Delta<t<0) \tag{33}$$

$$V_{triangular}(t)=\frac{2a}{\Delta}e^{-(t+\Delta)/\tau}\left(2e^{\Delta/2\tau}-1\right),(-\Delta/2<t<0) \tag{34}$$

Then, the initial values of the different excitation responses are obtained as:

$$V_{square}(-\Delta)=\lim_{t\to-\Delta}V_{square}(t)=\frac{a}{\tau} \tag{35}$$

$$V_{trapezoidal}(-\Delta+\Delta_1)=\lim_{t\to-\Delta+\Delta_1}V_{trapezoidal}(t)=\frac{a}{\Delta_1}(1-e^{-\Delta_1/\tau}) \tag{36}$$

$$V_{half\text{-}sine}(-\Delta)=\lim_{t\to-\Delta}V_{half\text{-}sine}(t)=-\frac{\pi a}{\Delta} \tag{37}$$

$$V_{triangular}(-\Delta/2)=\lim_{t\to-\Delta/2}V_{triangular}(t)=\frac{2a}{\Delta}\left(2-e^{-\Delta/2\tau}\right) \tag{38}$$

By normalizing (35) - (38) on $-a/\Delta$, the on-time initial response value varies with τ/Δ as shown in Figure 6, where the ratio of the edge width and the pulse width of Trapezoidal 1 and Trapezoidal 2 are 0.1 and 0.2, respectively.

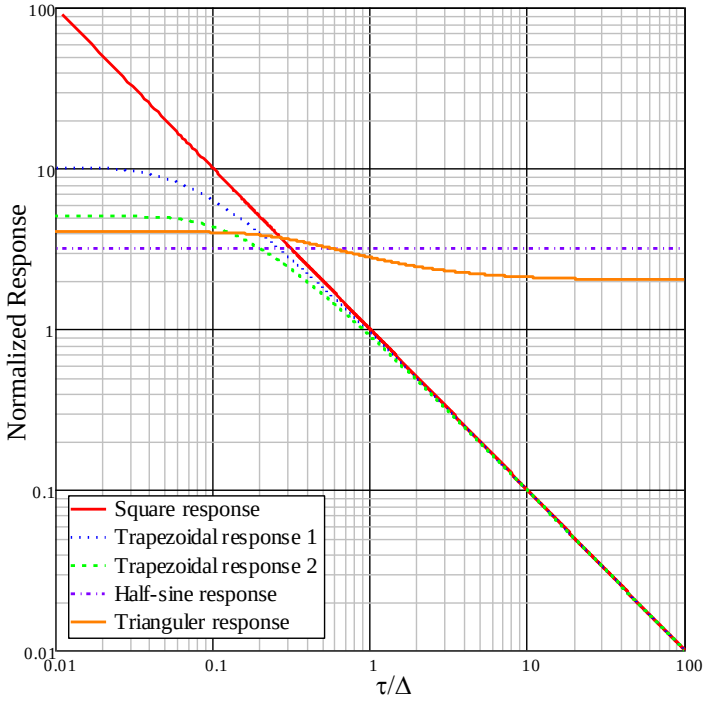

Fig.6. Initial Value of On-Time Response

4.3 Discussion of the on-Time Initial Response Value

(1) When τ/Δ is small ($\tau/\Delta<0.1$), the response amplitude of the square excitation is largest and the response amplitude of the trapezoidal excitation is smaller than that of the square excitation but greater than that of the triangular excitation and the half-sine excitation.

The responses of the trapezoidal excitation, triangular excitation, and half-sine excitation tend to be constant and do not change with the time constant. The response amplitude of the trapezoidal excitation increases with an increase in the slope of the rising edge.

By comparing (20) - (21) with (35) - (36), it can be found that in the low-conductivity region, the off-time response of the trapezoidal wave excitation is the same as the on-time response amplitude; however, the on-time acquisition requires the elimination of the first field and the on-time acquisition noise is greater than the off-time acquisition noise [9]. Therefore, the square excitation and the trapezoidal excitation are not suitable for on-time signal acquisition.

(2) When τ/Δ is large ($\tau/\Delta>1$), the trapezoidal excitation response and the square excitation response are less than the triangular excitation response and the half-sine excitation response. The square excitation response and the trapezoidal excitation response decrease with the time constant. It can be seen that the responses of the trapezoidal and the square excitation will decrease with an increase in the conductivity during on-time; therefore, the trapezoidal and square excitation sources are not suitable for detecting high-conductivity targets.

The amplitude of the half-sine excitation response remains constant regardless of the time constant. When $\tau/\Delta>1$, the response amplitude of the triangular excitation gradually decreases to half the amplitude of the low conductivity and remains constant. Therefore, the triangular and half-sine on-time signals can detect low-conductivity targets. The advantage of a half-sine wave is that it is easy to obtain a large peak magnetic moment for deep detection. The advantage of the triangular wave is that the primary field response is simple and is suitable for shallow low-resistance detection as well as early signal acquisition and processing. In addition, since the excitation responses of the triangular wave and the half-sine wave are less affected by the value of τ, the excitation source frequency can be appropriately increased to increase the number of signal superimpositions, thereby improving the signal-to-noise ratio and the spatial resolution.

5. On-Time and Off-Time Full Response Comparison

In the above section, the principle of the initial response values during on-time and off-time has been discussed respectively. However, the principle of the whole time-domain response has not be fully revealed yet. In this section, three more examples are taken, which are the triangular excitation used by AeroTEM, the half-sine excitation used by MegaTEM, and the trapezoidal excitation used by VTEM. Through average samples in various periods over off-time and on-time, multi-channel responses normalized on $-a/\Delta$ are obtained and analyzed.

Figure 7 and Figure 8 are the curves of the normalized response of the triangular and half sine energies with τ/Δ. It can be seen from the figures that the on-time response of the triangular and half-sine excitation on high conductivity orebodies is much greater than that of the off-time, however the on-time response of the triangular and half-sine excitation on the low conductivity orebodies is almost the same as the off-time response. When detecting high conductivity target bodies, the response of the triangular excitation tends to a same constant value at different channels, while the response of the half-sine excitation tends to be different, especially that responses near the start and end positions of the excitation waveform are high. By comparing Figure 9 (a) and Figure 9 (b), it can be found that response of the on-time trapezoidal wave excitation is almost the same as the off-time one, regardless of the ore's conductivity is high or low. The above principles are consistent with the results in [18] using the uniform half-space model. Moreover, the on-time response in Figure 7 is consistent with the experimental data in [19].

According to the above analysis, it can be proved that the free space loop coil model can reflect the response of on-time period. Considering that the airborne TDEM noise during the on-time is much higher than off-time, the use of off-time acquisition in the detection of low-conductivity ore bodies can get a higher signal-to-noise ratio. The on-time responses of half-sine and triangular excitation are sensitive to high τ/Δ ore body, so a high response signal can be obtained by reducing the pulse width Δ. A low Δ means a high excitation frequency, and a high frequency also means an increase in the number of receiving signal overlaps, which is much beneficial for noise reducing, ratio improving, and exploration deepening.

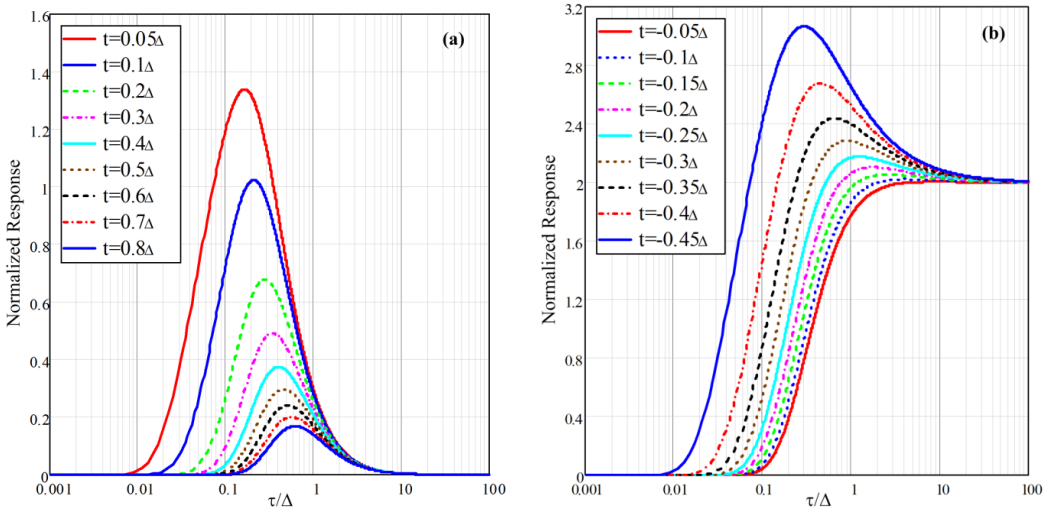

Fig.7. Triangular Excitation Normalized Response for the 9 Channels Vs. T/Δ.

Where, A: Off-Time Response, B: On-Time Response

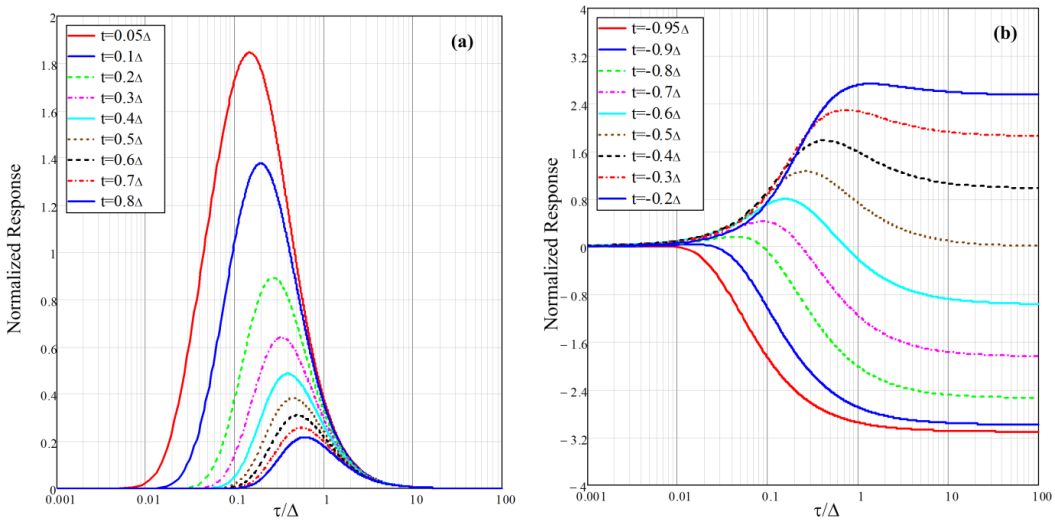

Fig.8. Half-sine Excitation Normalized Response for the 10 Channels Vs. T/Δ.

Where, A: Off-Time Response, B:On-Time Response

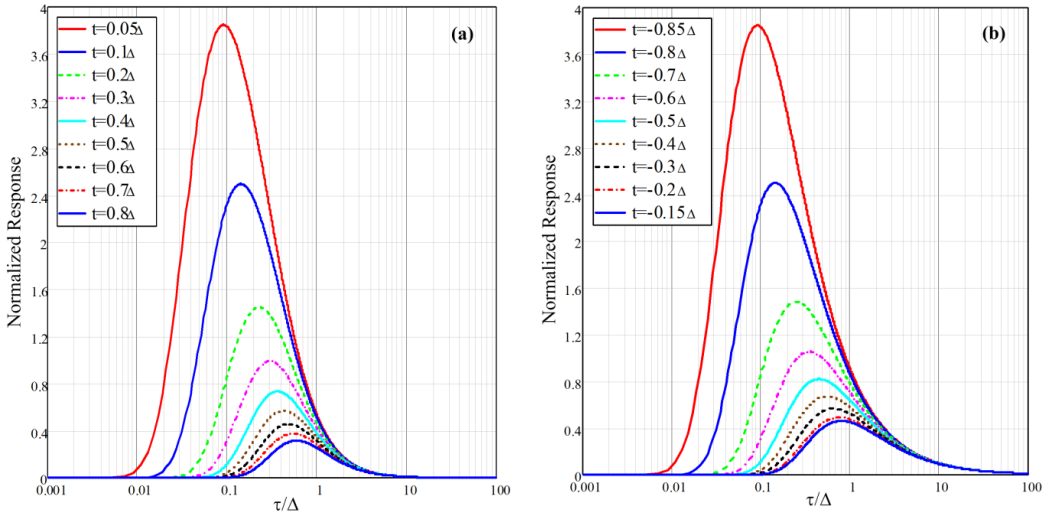

Fig.9. Trapezoidal Excitation Normalized Response for 9 Channels Vs. T/Δ,

Where A: Off-Time Response, B: On-Time Response

Conclusions

The response principle given by the free space conductive loop coil model has a simple mathematical expression, which easily reveals the characteristics of the off-time and on-time responses of different excitation waveforms. The conclusions provide general and significant guiding principles.

The square excitation and the trapezoidal excitation are suitable for off-time acquisition and are not suitable for on-time acquisition. In the low-conductivity region, the on-time responses of

the square excitation and trapezoidal excitation are comparable to the off-time response amplitude but the on-time acquisition noise is greater than the off-time acquisition noise; therefore, a higher signal-to-noise ratio can be obtained for the off-time acquisition.

Ground-based TDEM systems typically use square wave or trapezoidal wave excitation for detection but in high-conductivity regions, the on-time and off-time signals will decrease with an increase in the conductivity; therefore, the detection capability for high-conductivity targets and the resolution will decrease.

The half-sine excitation and triangular excitation are suitable for on-time acquisition. In the high-conductivity region, the response amplitude of the triangular excitation and the half-sine excitation hardly decreases with an increase in the conductivity; therefore, the high-conductivity target can be detected and the target's resolution can be improved. In addition, by improving the transmitting magnetic moment, a strong off-time signal can be obtained and the off-time response signal-to-noise ratio and detection depth can be improved.

In the off-time, the trapezoidal, triangular, and half-sine excitations have the optimal pulse width, that is, when $\tau/\Delta=0.4$, the system can obtain the optimal response signal. Therefore, for targets with different conductivity, the best excitation source frequency needs to be chosen for the measurements. The square excitation does not have the best pulse width and the greater the pulse width, the greater the signal amplitude is. In the on-time, since the response amplitude of the half-sine excitation and the triangular excitation is not related to the target's conductivity, the frequency of the excitation source can be increased to increase the number of signal superposition times, thus improving the signal-to-noise ratio and the spatial resolution of the system.

References

1. D. Fountain, Airborne electronmagnetic systems 50 years of development, 1998, Exploration Geophysics, vol. 29, no. 2, pp.1-11.
2. C.C. Yin, B. Zhang, Y.H. Liu, et al, Review on airborne EM technology and developments, 2015, Chinese J. Geophysics, vol. 58, no. 8, pp. 2637-2653.
3. A.A. Pfaffhuber, E. Grimstad, U. Domaas, M. Marchetti, Airborne EM mapping of rockslides and tunneling hazards, 2010, The Leading Edge, vol. 29, no. 8, pp. 956-959.
4. M.A. Vallée, R.S. Smith, P. Keating, Metalliferous mining geophysics - State of the art after a decade in the new millennium, 2011, Geophysics, vol. 76, no. 4, pp. W31-W50.

5. V. Sapia, G. Oldenborger, A. Viezzoli, M. Marchetti, Incorporating ancillary data into the inversion of airborne time-domain electromagnetic data for hydrogeological applications, 2014, Journal of Applied Geophysics, vol. 104, no. 5, pp. 35-43.
6. S. Chandra, S. Ahmed, E. Auken, J.B. Pedersen, A. Singh, 3D aquifer mapping employing airborne geophysics to meet India's water future, 2016, The Leading Edge, vol. 35, no. 9, pp.770-774.
7. R.S. Smith, A.P. Annan, Using an induction coil sensor to indirectly measure the B-field response in the bandwidth of the transient electromagnetic method, 2000, Geophysics, vol. 65, no. 5, pp.1489-1494.
8. R.S. Smith, J. Lemieux, R. Smith, J. Lemieux, Examples showing characteristics of the MEGATEM airborne electromagnetic system, 2009, ASEG Extended Abstracts 20th Geophysical Conference, pp.1-10.
9. J. Rudd, The AeroTEM HD Advantage, 2011, 12th International Congress of the Brazilian Geophysical Society & EXPOGEF, Rio de Janeiro, Brazil, pp. 190-194.
10. J. Lemieux, Airborne Electromagnetic Systems – State of the Art and Future Directions, 2015, CSEG Recorder, vol. 40, no. 6, pp. 38-49.
11. D.V. Fitterman, W.L. Anderson, Effect of transmitter turn-off time on transient soundings, 1987, Geoexploration, vol. 24, no. 2, pp. 131-146.
12. Y.J. Ji, J. Lin, S.B. Yu, Z. Wang, J. Wang, A study on solution of transient electromagnetic response during transmitting current turn-off in the ATTEM system, 2006, Chinese Journal of Geophysics, vol. 49, no. 6, pp.1884-1890.
13. S.L. Wang, C.C. Yin, J. Lin, Bipolar square-wave current source for transient electromagnetic systems based on constant shutdown time, 2016, Review of Scientific Instruments, vol. 87, no. 3, pp.1-9.
14. G. Hodges, T. Chen, Geobandwidth: comparing time domain electromagnetic waveforms with a wire loop model, 2014, Exploration Geophysics, vol.46, no.1, pp. 58-63.
15. G. Liu, Effect of transmitter current waveform on airborne TEM response, 1998, Exploration Geophysics, vol. 29, no. 2, pp. 35-41.
16. G.F. West, J.C. Macnae, Physics of the Electromagnetic Induction Exploration Method, 1991, Electromagnetic Methods in Applied Geophysics, pp. 5-46.
17. F.S. Grant, G.F West, Interpretation Theory in Applied Geophysics, 1965, McGraw-Hill Book Company.

18. C.C. Yin, X.Y. Ren, Y.H. Liu, et al, Exploration capability of airborne TEM systems for typical targets in the subsurface, 2015, Chinese J. Geophysics, vol. 58, no. 9, pp. 3370-3379.
19. R.S. Smith, G. Hodges, J. Lemieux, Case histories illustrating the characteristics of the HeliGEOTEM system, 2009, Exploration Geophysics, vol. 40, no. 3, pp. 246-256.